4 $^{40}Ar/^{39}Ar$ GEOCHRONOLOGY OF SELECTED SAMPLES IN THE KHEIS- AND KAKAMAS TERRANES.

4.1 INTRODUCTION

The age of deformation of the Kheis Terrane remains uncertain. It was always thought to be of Eburnean (~1.8Ga) age (Cornell *et al*., 1998 and Moen, 1999). However, recent unpublished U-Pb SHRIMP age of 1290Ma (Moen, unpublished data) for the Kalkwerf Gneiss which is deformed together with the rocks of the Keis Supergroup into the Kheis Terrane suggest that deformation that formed the Kheis Terrane may be much younger than thought earlier.

A study of neomorphic mica from both the Kheis- and Kakamas Terranes was undertaken to address this problem. Here, we present laser incremental heating $^{40}Ar/^{39}Ar$ analyses of metamorphic muscovite from the Korannaland Group of the Kakamas Terrane and the Keis Supergroup of the Kheis Terrane (Figure 4.2) that provide constraints regarding the age of the Kheis Terrane as well as the timing of the collision between the Kheis- and Kakamas Terranes during the formation of the NNMP.

4.2 SAMPLE LOCATIONS

Three samples were carefully collected for $^{40}Ar/^{39}Ar$ analyses of metamorphic muscovite. One sample was taken from the Goedehoop Formation and the other two come from the Opwag- and Skurweberg Formations of the Groblershoop Group of the Keis Supergroup (Figure 4.3).

4.2.1 GOEDEHOOP FORMATION OF THE KORANNALAND GROUP

The pink granitic Kokerberg gneiss is directly overlain by at least three upward coarsening cycles of the flat laminated amphibolites, calc-silicates and phyllites of the Puntsit Formation. The uppermost cycle of the Puntsit Formation is in turn overlain by the thick medium to

poorly sorted quartzites and arkosic quartzites of the Goedehoop Formation. Although classified as a part of the NNMP, one of the distinguishing and striking features of the Goedehoop Formation is the low strain nature of the quartzites. Sedimentary structures are well preserved and up to 50 cm high planar- and trough cross-bedding are common. A well developed foliation defined by authigenic muscovite occur semi-parallel to the sedimentary layering in the quartzites. These quartzites were sampled as sample PH-33 (Figure 4.3).

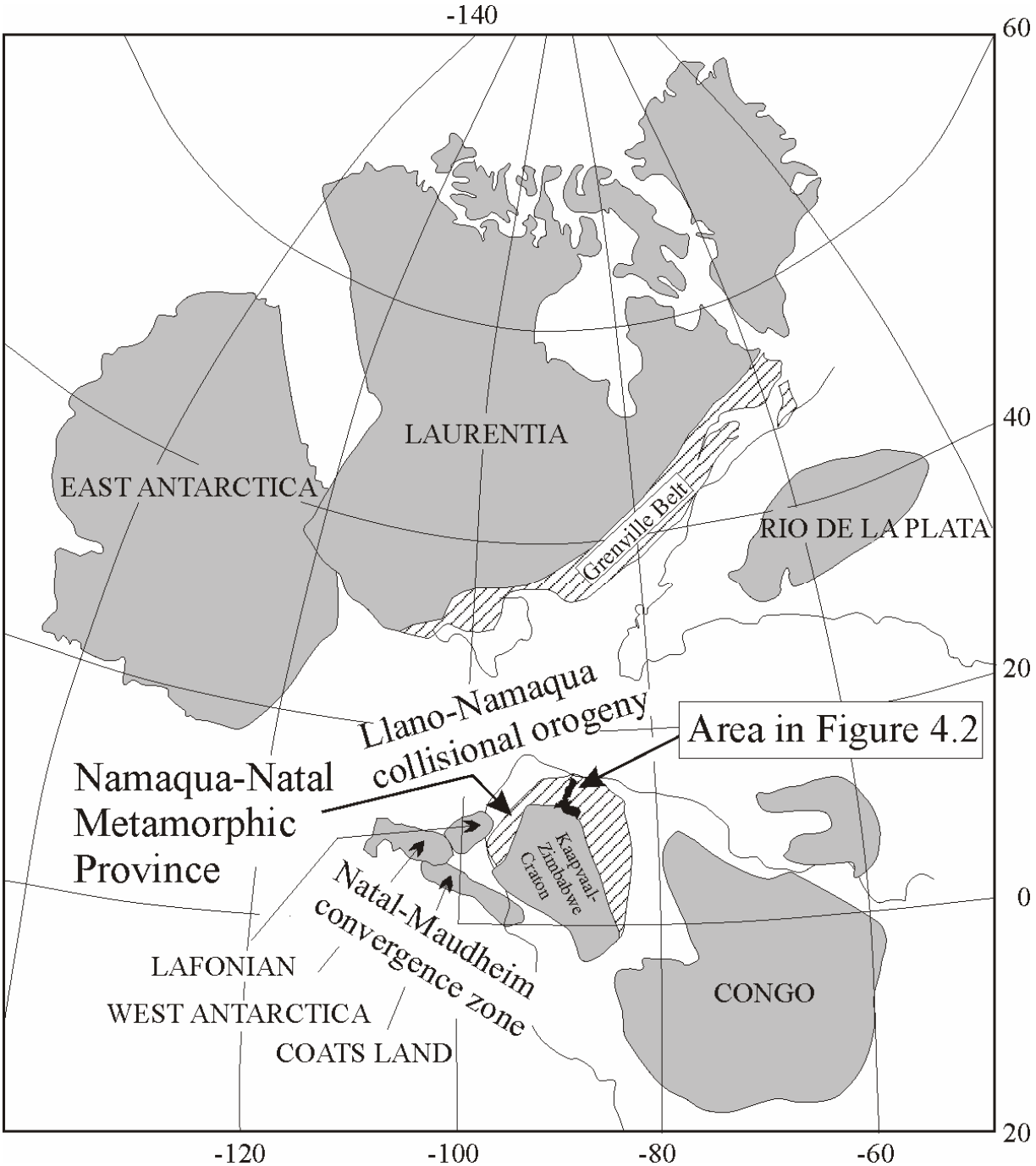

Figure 4.1: The location of the Kalahari and Laurentia cratons at ~1100Ma according to the reconstruction of Dalziel *et al*. (2000) using present day North American coordinates (Modified after Dalziel *et al*., 2000).

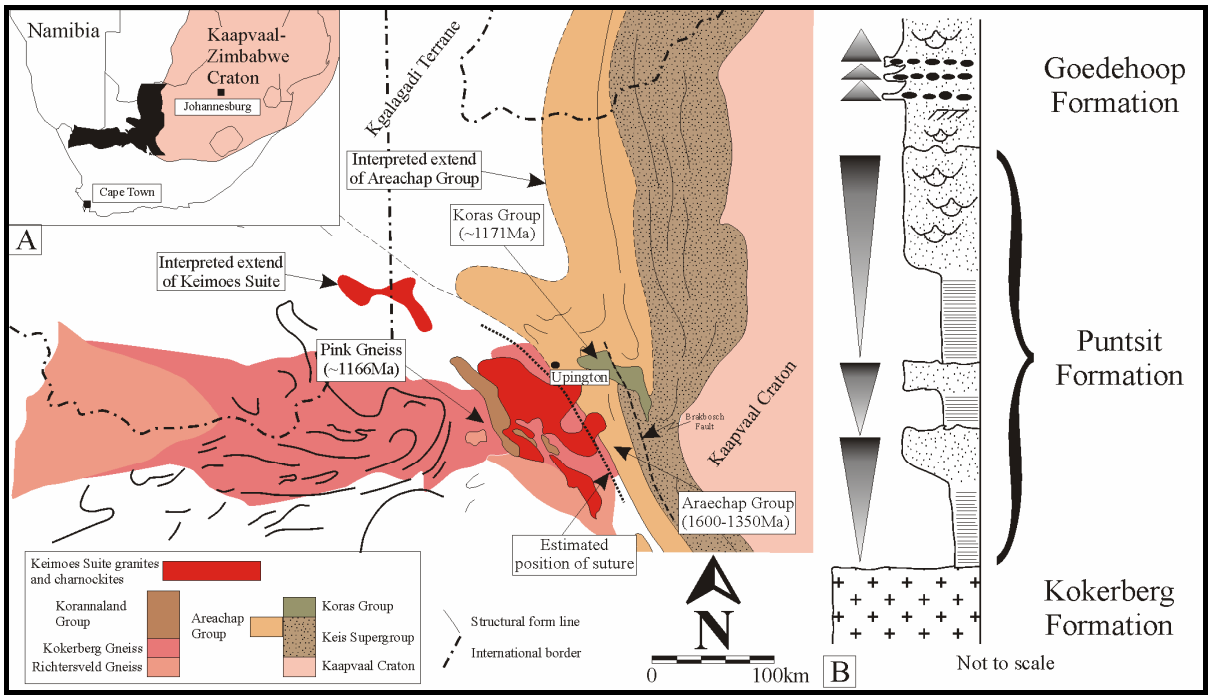

Figure 4.2: A) Subdivision of the Namaquan part of the NNMP into crustal terranes. Note the location of the Goedehoop Formation and the interpreted extent of the Areachap Group. **B)** Sketch profile of the nonconformable contact between the Kokerberg gneiss and the overlying metasedimentary rocks of the Puntsit and Goedehoop Formations.

Sample PH-33 is composed of angular to subrounded framework grains of monocrystalline quartz with concavo-convex to sutured grain boundaries, which appear to be somewhat elongated and which are separated from each other by neomorphic muscovite flakes (160–600 µm). These muscovite flakes also exhibit a weak orientation sub-parallel to the apparent elongation direction of the quartz. Some subhedral to rounded opaque ore minerals (140-200µm) are associated with the muscovite flakes. The framework grains and matrix of fine-grained quartz (<30µm) are cemented by very fine-grained quartz. Secondary chlorite (<30µm) replace some framework and matrix quartz along their grain boundaries. Three muscovite clusters and single crystals were separated from sample PH-33 for $^{40}Ar/^{39}Ar$ analyses.

4.2.2 GROBLERSHOOP GROUP OF THE KEIS SUPERGROUP

Sample PU-4, a micaceous quartz-schist, was taken from the Opwag Formation to the northwest of Groblershoop (Figure 4.3). It is composed of subangular to well-rounded monocrystalline quartz framework grains (80–400µm) that occur with concavo-convex contacts toward each other and show undulose extinction.

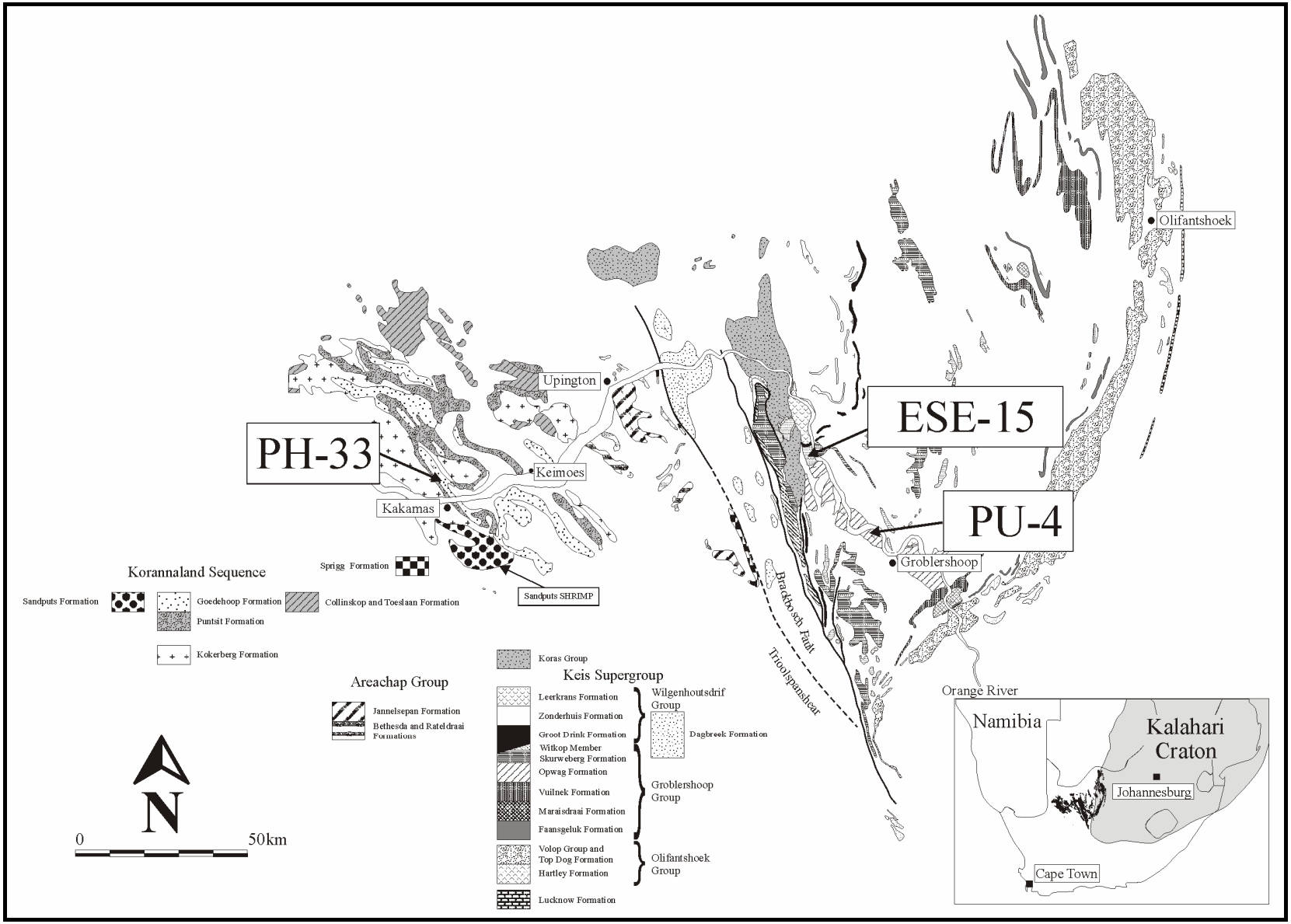

Figure 4.3: Localities for the samples taken from the Goedehoop Formation (PH-33) of the Korannaland Group and the Opwag Formation (PU-4) and the Skurweberg Formation (ESE-15) of the Keis Supergroup.

Interstices between the framework grains are filled by fine-grained quartz cement, composed of subhedral quartz grains (<30 μm in size). Neomorphic mica flakes (180–250 μm long) define a weakly developed schistosity developed in this sample.

Sample ESE-15 was taken from the Skurweberg Formation of the Groblershoop Group to the northwest of Groblershoop (Figure 4.3). It is composed of elongated framework grains of quartz (200-400μm) with concavo-convex grain boundaries exhibiting undulose extinction. In a few cases dust rims are preserved, indicating mostly rounded grains before deformation. A strong metamorphic overprint is defined by the presence of a large amount of secondary, colourless, 100 -600μm long flakes of mica, which are orientated semi-parallel to the elongated quartz grains. Some rounded (~40μm) and subhedral opaque ore minerals are also present.

Two muscovite flake samples from the Opwag Formation and three from the Skurweberg Formation were separated for $^{40}Ar/^{39}Ar$ analyses.

4.3 $^{40}Ar/^{39}Ar$ GEOCHRONOLOGY

Muscovite samples were irradiated for 14 hours at the CLICIT facility in the Oregon State University Radiation Centre TRIGA Reactor and dated by the laser incremental heating method at UQ-AGES (University of Queensland Argon Geochronology in Earth Sciences laboratory), following the procedures detailed in Vasconcelos *et al*. (2002). Fish Canyon sanidine irradiated with the samples yield J factors of 0.003702±0.00000355 and 0.003727±0.000004; other irradiation correction factors are: $(2.64\pm0.02)*10^{-4}$ for $(^{36}Ar/^{37}Ar)_{Ca}$, $(7.04\pm0.06)*10^{-4}$ for $(^{39}Ar/^{37}Ar)_{Ca}$ and $(8\pm3)*10^{-4}$ for $(^{40}Ar/^{36}Ar)_{K}$. air pipettes and full system blanks were analysed before and after each grain, yielding $^{40}Ar/^{36}Ar$ discrimination values of 1.0075±0.0018. All dates are reported using $5.543*10^{-10}a^{-1}$ as the total decay constant for ^{40}K (Steiger and Jäger, 1978).

The results illustrated in Figure 4.4 and summarized in Table 4.1, yield well-defined plateau ages ranging between 1111±3 to 1121±3Ma for the muscovites from the Goedehoop Formation (Figure 4.4B). A probability density plot for all steps analysed yield a most probable age peak at 1116Ma, with a weighted mean average of 1113±3Ma (Figure 4.4A). It

is important to recognise the total lack of a Pan-African overprint in the analysed muscovite flakes and clusters.

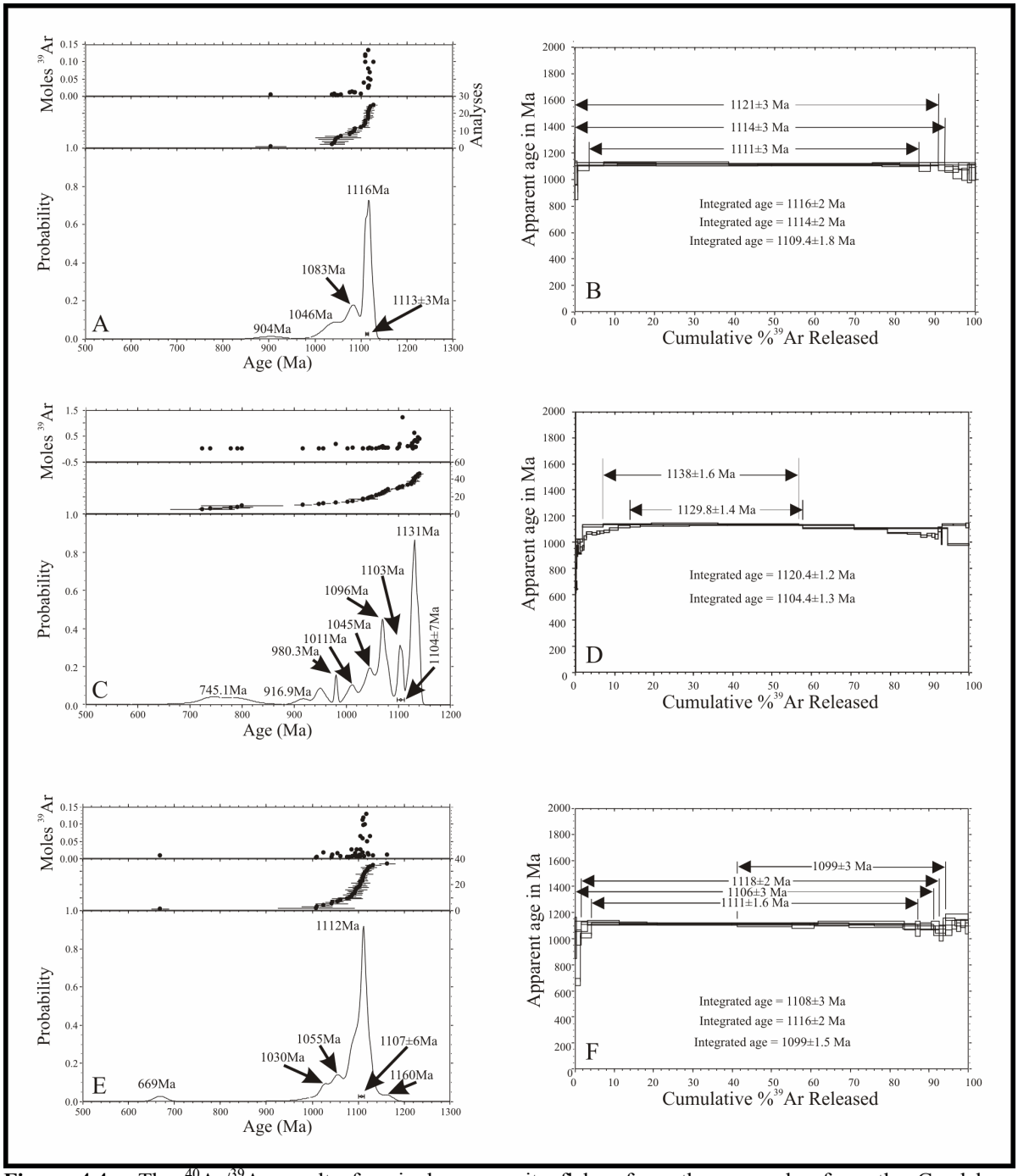

Figure 4.4: The $^{40}Ar/^{39}Ar$ results for single muscovite flakes from three samples from the Goedehoop Formation (A and B) and the Kheis Terrane (sample PU-4: C and D and sample ESE-15: E and F).

The muscovite flakes from the Kheis Terrane yielded slightly older but similar probable ages of 1131Ma and 1112Ma as well as weighted mean averages of 1104±7Ma (PU-4) and 1107±6Ma (ESE-15) respectively (Figure 4.4C and 4.4E). Plateau ages vary from between

1104.4±1.3Ma and 1120.4±1.2Ma for PU-4 and 1099±3Ma and 1116±2Ma for ESE-15 respectively (Figure 4.4D and F).

Table 4.1: $^{40}Ar/^{39}Ar$ age dating results for the 3 muscovite samples from the Goedehoop Formation (PH-33) and sedimentary rocks from the Kheis Terrane (PU-4 and ESE-15).

Sample	*$^{40}Ar/^{39}Ar$*	*$^{38}Ar/^{39}Ar$*	*$^{37}Ar/^{39}Ar$*	*$^{36}Ar/^{39}Ar$*	*$^{40}Ar^*/^{39}Ar$*	*% Rad*	*Age (Ma)*	*± (Ma)*
Sample PH-33								
Flake 1								
PH-33	*235.44*	*2.12E-02*	*0.00E+00*	*1.83E-02*	*230.04*	*97.70*	***1117.00***	***6.46***
PH-33	*234.51*	*1.37E-02*	*0.00E+00*	*4.95E-03*	*233.04*	*99.40*	***1127.85***	***3.61***
PH-33	*230.92*	*1.30E-02*	*0.00E+00*	*2.72E-03*	*230.11*	*99.70*	***1117.27***	***2.81***
PH-33	*230.14*	*1.55E-02*	*0.00E+00*	*-1.23E-03*	*230.51*	*100.20*	***1118.69***	***6.24***
PH-33	*227.18*	*2.45E-02*	*0.00E+00*	*1.72E-02*	*222.10*	*97.80*	***1088.04***	***10.52***
PH-33	*221.06*	*2.71E-02*	*0.00E+00*	*3.73E-02*	*210.03*	*95.00*	***1043.07***	***17.42***
PH-33	*224.04*	*1.25E-02*	*0.00E+00*	*5.20E-02*	*208.68*	*93.10*	***1037.97***	***22.26***
PH-33	*230.47*	*1.60E-02*	*0.00E+00*	*6.67E-02*	*210.76*	*91.40*	***1045.83***	***33.67***
PH-33	*229.00*	*8.67E-03*	*0.00E+00*	*5.23E-02*	*213.54*	*93.20*	***1056.25***	***29.82***
Flake 2								
PH-33	*198.26*	*5.28E-02*	*1.97E-01*	*8.08E-02*	*174.43*	*88.00*	***903.54***	***28.20***
PH-33	*236.11*	*2.77E-02*	*1.14E-01*	*4.92E-02*	*221.61*	*93.80*	***1086.22***	***10.62***
PH-33	*232.05*	*1.41E-02*	*0.00E+00*	*3.89E-03*	*230.90*	*99.50*	***1120.12***	***3.92***
PH-33	*229.13*	*1.25E-02*	*0.00E+00*	*3.34E-03*	*228.14*	*99.60*	***1110.12***	***3.32***
PH-33	*229.01*	*1.38E-02*	*1.51E-03*	*3.34E-03*	*228.02*	*99.60*	***1109.68***	***3.18***
PH-33	*229.80*	*1.63E-02*	*1.88E-02*	*9.18E-03*	*227.09*	*98.80*	***1106.31***	***4.35***
PH-33	*230.94*	*1.36E-02*	*1.28E-01*	*3.67E-02*	*220.12*	*95.30*	***1080.74***	***10.55***
PH-33	*233.80*	*1.30E-02*	*7.18E-04*	*8.88E-03*	*231.17*	*98.90*	***1121.10***	***4.55***
Flake3								
PH-33	*209.89*	*9.57E-03*	*9.30E-02*	*-7.80E-03*	*212.22*	*101.10*	***1051.30***	***44.36***
PH-33	*230.09*	*1.56E-02*	*0.00E+00*	*3.25E-04*	*229.99*	*100.00*	***1116.83***	***6.11***
PH-33	*227.72*	*1.21E-02*	*0.00E+00*	*-9.18E-04*	*227.99*	*100.10*	***1109.57***	***3.53***
PH-33	*230.45*	*1.43E-02*	*0.00E+00*	*2.05E-03*	*229.84*	*99.70*	***1116.29***	***3.48***
PH-33	*229.91*	*1.75E-02*	*0.00E+00*	*-3.36E-04*	*230.01*	*100.00*	***1116.90***	***4.61***
PH-33	*227.37*	*2.36E-02*	*0.00E+00*	*2.84E-02*	*218.98*	*96.30*	***1076.53***	***11.70***
PH-33	*226.34*	*1.74E-02*	*0.00E+00*	*2.50E-03*	*225.60*	*99.70*	***1100.86***	***15.12***
PH-33	*224.20*	*1.82E-02*	*0.00E+00*	*4.72E-02*	*210.24*	*93.80*	***1043.86***	***23.91***
Sample PU-4								
Flake 1								
PU-4	*188.69*	*-3.38E+00*	*5.02E+00*	*9.27E+00*	*-2559.75*	*%-1351.8*	***0.00***	***7455.99***
PU-4	*-67.47*	*1.33E+00*	*0.00E+00*	*-4.36E+00*	*1221.27*	*%-1810.1*	***3082.42***	***3664.83***
PU-4	*139.32*	*-4.92E-02*	*0.00E+00*	*-4.22E-01*	*263.95*	*189.50*	***1229.76***	***1292.64***
PU-4	*304.22*	*1.17E+00*	*6.07E+00*	*3.26E+00*	*-661.28*	*%-216.4*	***0.00***	***3711.70***
PU-4	*172.45*	*6.95E-02*	*4.82E-01*	*6.78E-01*	*-27.85*	*-16.10*	***-196.33***	***549.65***
PU-4	*169.66*	*6.06E-02*	*0.00E+00*	*3.59E-01*	*63.62*	*37.50*	***381.54***	***189.42***
PU-4	*163.28*	*2.56E-02*	*0.00E+00*	*4.23E-02*	*150.79*	*92.30*	***800.18***	***74.51***
PU-4	*160.96*	*3.85E-02*	*3.36E-02*	*9.34E-02*	*133.36*	*82.90*	***723.91***	***58.04***
PU-4	*152.26*	*3.14E-02*	*0.00E+00*	*2.21E-02*	*145.73*	*95.70*	***778.38***	***32.63***
PU-4	*153.08*	*3.16E-02*	*0.00E+00*	*1.42E-02*	*148.89*	*97.30*	***792.03***	***24.79***

Sample	$^{40}Ar/^{39}Ar$	$^{38}Ar/^{39}Ar$	$^{37}Ar/^{39}Ar$	$^{36}Ar/^{39}Ar$	$^{40}Ar^{*}/^{39}Ar$	% Rad	Age (Ma)	± (Ma)
PU-4	187.95	2.70E-02	0.00E+00	3.01E-02	179.05	95.30	**917.44**	**12.92**
PU-4	204.60	1.29E-02	0.00E+00	1.26E-02	200.87	98.20	**1003.01**	**8.65**
PU-4	193.01	1.45E-02	5.02E-03	2.15E-02	186.66	96.70	**947.72**	**7.21**
PU-4	195.34	1.97E-02	0.00E+00	2.19E-02	188.88	96.70	**956.47**	**9.85**
PU-4	211.54	1.12E-02	0.00E+00	1.04E-02	208.46	98.50	**1031.86**	**7.58**
PU-4	221.41	1.14E-02	2.79E-03	8.59E-03	218.87	98.90	**1070.67**	**4.99**
PU-4	218.28	1.18E-02	0.00E+00	4.20E-03	217.04	99.40	**1063.89**	**5.02**
PU-4	220.84	1.36E-02	4.81E-03	2.62E-03	220.07	99.60	**1075.07**	**5.81**
PU-4	220.74	1.05E-02	2.79E-03	1.51E-03	220.29	99.80	**1075.91**	**5.19**
PU-4	222.69	1.14E-02	9.67E-03	3.62E-03	221.62	99.50	**1080.78**	**4.67**
PU-4	227.77	1.18E-02	7.96E-03	1.86E-03	227.23	99.80	**1101.23**	**3.65**
PU-4	231.71	1.05E-02	8.17E-03	-4.15E-04	231.83	100.10	**1117.85**	**3.67**
PU-4	233.00	1.21E-02	0.00E+00	-2.90E-03	233.86	100.40	**1125.12**	**3.51**
PU-4	234.15	1.13E-02	1.24E-02	-3.55E-04	234.26	100.00	**1126.57**	**2.61**
PU-4	234.44	1.12E-02	6.19E-03	2.75E-05	234.43	100.00	**1127.17**	**2.71**
PU-4	235.64	1.18E-02	8.93E-03	-4.55E-04	235.77	100.10	**1131.97**	**2.62**
PU-4	235.64	1.20E-02	1.20E-02	1.91E-04	235.58	100.00	**1131.29**	**2.23**
PU-4	229.17	1.16E-02	3.65E-02	4.31E-04	229.05	99.90	**1107.84**	**2.24**
PU-4	195.51	1.26E-02	1.36E-01	1.97E-03	194.96	99.70	**980.20**	**2.68**
Flake 2								
PU-4	146.01	-1.45E-02	0.00E+00	3.15E-02	136.71	93.60	**738.79**	**17.76**
PU-4	209.52	1.36E-02	1.85E-02	2.08E-02	203.39	97.10	**1012.62**	**6.18**
PU-4	234.58	1.23E-02	1.27E-02	2.81E-03	233.75	99.60	**1124.75**	**3.49**
PU-4	237.34	1.24E-02	4.14E-03	1.41E-03	236.93	99.80	**1136.08**	**2.60**
PU-4	238.51	1.21E-02	4.26E-03	3.70E-04	238.40	100.00	**1141.31**	**2.41**
PU-4	237.70	1.24E-02	7.61E-03	8.34E-04	237.45	99.90	**1137.95**	**2.45**
PU-4	235.85	1.15E-02	2.05E-02	1.36E-03	235.45	99.80	**1130.82**	**2.45**
PU-4	228.34	1.21E-02	2.31E-02	2.12E-03	227.71	99.70	**1103.00**	**2.64**
PU-4	220.10	1.23E-02	2.59E-02	4.89E-03	218.66	99.30	**1069.91**	**2.97**
PU-4	218.69	1.36E-02	3.99E-02	2.44E-03	217.98	99.70	**1067.36**	**3.63**
PU-4	215.31	1.85E-02	8.42E-02	1.19E-02	211.82	98.40	**1044.46**	**5.24**
PU-4	220.14	1.73E-02	1.44E-01	1.61E-02	215.40	97.80	**1057.82**	**5.79**
PU-4	221.87	2.24E-02	1.57E-01	2.97E-02	213.14	96.10	**1049.38**	**7.76**
PU-4	224.98	1.85E-02	1.80E-01	4.65E-02	211.30	93.90	**1042.50**	**9.12**
PU-4	234.17	1.89E-02	4.35E-02	2.61E-02	226.47	96.70	**1098.50**	**8.48**
PU-4	228.16	4.19E-02	2.66E-02	6.64E-02	208.56	91.40	**1032.20**	**23.81**
PU-4	237.43	1.08E-02	2.69E-02	4.57E-03	236.08	99.40	**1133.08**	**4.06**
PU-4	237.72	1.44E-02	2.94E-02	4.20E-03	236.48	99.50	**1134.50**	**4.27**
PU-4	240.99	2.49E-02	0.00E+00	2.13E-02	234.71	97.40	**1128.18**	**8.22**
Sample ESE-15								
Flake 1								
ESE-15	124.85	3.56E-02	0.00E+00	1.21E-02	121.28	97.10	**669.05**	**14.03**
ESE-15	212.64	2.21E-02	0.00E+00	1.98E-02	206.78	97.20	**1025.50**	**8.27**
ESE-15	231.36	1.37E-02	0.00E+00	1.11E-03	231.03	99.90	**1114.97**	**3.31**
ESE-15	229.39	1.37E-02	0.00E+00	-1.50E-03	229.83	100.20	**1110.65**	**3.13**
ESE-15	229.91	1.34E-02	3.48E-03	-4.67E-04	230.05	100.10	**1111.45**	**2.89**
ESE-15	229.74	1.42E-02	1.27E-01	-6.42E-04	229.96	100.10	**1111.11**	**3.15**
ESE-15	228.67	1.48E-02	7.04E-03	8.76E-04	228.42	99.90	**1105.55**	**3.49**

Sample	$^{40}Ar/^{39}Ar$	$^{38}Ar/^{39}Ar$	$^{37}Ar/^{39}Ar$	$^{36}Ar/^{39}Ar$	$^{40}Ar^{*}/^{39}Ar$	% Rad	Age (Ma)	± (Ma)
ESE-15	225.76	1.82E-02	0.00E+00	9.75E-03	222.88	98.70	**1085.40**	**5.55**
ESE-15	220.93	1.69E-02	4.09E-02	2.08E-02	214.78	97.20	**1055.53**	**7.90**
ESE-15	220.15	3.61E-02	3.51E-02	2.87E-02	211.68	96.10	**1043.94**	**10.52**
ESE-15	224.40	4.37E-02	0.00E+00	-1.31E-02	228.26	101.70	**1104.99**	**16.70**
ESE-15	227.83	5.01E-02	0.00E+00	1.54E-02	223.28	98.00	**1086.87**	**16.51**
ESE-15	236.33	3.13E-02	2.48E-02	1.92E-02	230.67	97.60	**1113.69**	**15.17**
ESE-15	229.86	4.75E-02	0.00E+00	2.83E-02	221.51	96.40	**1080.37**	**20.50**
Flake 2								
ESE-15	260.92	-1.07E-02	0.00E+00	1.99E-01	202.22	77.50	**1008.15**	**79.31**
ESE-15	237.34	4.98E-02	1.36E-01	1.18E-01	202.59	85.30	**1009.58**	**29.11**
ESE-15	234.12	1.40E-02	0.00E+00	5.86E-03	232.39	99.30	**1119.87**	**4.24**
ESE-15	232.58	1.29E-02	0.00E+00	2.49E-03	231.85	99.70	**1117.92**	**3.09**
ESE-15	235.00	1.44E-02	0.00E+00	2.50E-03	234.26	99.70	**1126.56**	**4.10**
ESE-15	228.73	3.48E-02	0.00E+00	1.39E-02	224.61	98.20	**1091.71**	**13.46**
ESE-15	241.24	1.13E-02	0.00E+00	7.12E-02	220.21	91.30	**1075.59**	**28.65**
ESE-15	231.51	2.17E-02	0.00E+00	2.11E-02	225.27	97.30	**1094.10**	**13.60**
ESE-15	228.82	4.22E-02	0.00E+00	5.40E-03	227.22	99.30	**1101.20**	**17.62**
ESE-15	226.44	3.25E-02	0.00E+00	5.18E-02	211.14	93.20	**1041.91**	**30.13**
ESE-15	237.39	1.45E-02	0.00E+00	5.44E-03	235.78	99.30	**1131.99**	**13.26**
ESE-15	230.42	1.26E-02	0.00E+00	-9.95E-03	233.36	101.30	**1123.34**	**12.14**
Flake 3								
ESE-15	238.05	4.81E-02	6.19E-02	4.23E-02	225.56	94.70	**1095.19**	**18.89**
ESE-15	234.73	5.75E-03	0.00E+00	5.99E-03	232.96	99.20	**1121.90**	**8.81**
ESE-15	231.07	1.05E-02	0.00E+00	4.31E-03	229.79	99.40	**1110.52**	**4.13**
ESE-15	232.11	1.27E-02	0.00E+00	1.32E-02	228.20	98.30	**1104.77**	**6.04**
ESE-15	230.00	9.24E-03	0.00E+00	7.48E-03	227.79	99.00	**1103.27**	**10.85**
ESE-15	232.12	1.38E-02	0.00E+00	8.85E-03	229.50	98.90	**1109.47**	**7.23**
ESE-15	227.40	1.22E-02	0.00E+00	4.62E-03	226.03	99.40	**1096.88**	**5.49**
ESE-15	232.91	1.73E-02	0.00E+00	2.66E-02	225.06	96.60	**1093.34**	**9.48**
ESE-15	226.22	2.79E-02	0.00E+00	3.27E-02	216.57	95.70	**1062.17**	**18.09**
ESE-15	245.81	1.42E-02	0.00E+00	3.74E-03	244.70	99.60	**1163.55**	**12.57**

4.4 DISCUSSION

The measured age of the authigenic muscovite in the Goedehoop Formation indicate that the deposition of the Goedehoop Formation took place between ~1166Ma (the age of the Kokerberg gneiss) and ~1113Ma (average age obtained from the muscovite in the Goedehoop Formation). The absence of any 2000Ma to 3000Ma old zircon grains in the quartzites of the Goedehoop Formation (see previous chapter) suggest that deposition occurred when the depositional basin of the Korannaland Group and the western margin of the Kaapvaal-Zimbabwe Craton (consisting of the sedimentary rocks of the Kheis Terrane) were unconnected. Shortly after the deposition of the sedimentary rocks of the Puntsit- and

Goedehoop Formations of the Korannaland Group (about 50Ma later) a single event of deformation and metamorphism affected the Kakamas Terrane around ~1113Ma. This event may also be linked to the intrusion of the ~1100Ma Keimoes Suite of granitoids (Geringer *et al.*, 1988) into the rocks of the Kakamas Terrane. The chemical characteristics and I-type properties of the Keimoes granitoids resemble that of destructive margin type granites (Geringer *et al*., 1988) suggesting that the intrusion of the Keimoes Suite granitoids may be linked to the final stages of westward directed subduction associated with the collision of the Kaapvaal section of the Kaapvaal-Zimbabwe Craton with supracrustal material of the Kakamas and Richtersveld Terranes.

It has to be remembered that the exact meaning of the ~1113Ma age in the tectonic history of the Namaqua complex of the Namaqua-Natal Metamorphic Province is difficult to determine. This is mainly due to the uncertainties pertaining to the closure temperature of the muscovite analysed in these samples. Closure temperatures for various stable and radiogenic isotopes in minerals depend on many factors that include grain size, major element composition, fluid availability and thermal history (Zheng *et al*., 2003). Therefore, a unique closure temperature cannot be assigned for any given chemical element in any specific mineral. But for the purpose of this study it is assumed that the final collisional event took place soon after ~1113Ma.

Very important is the absence of any $^{40}Ar/^{39}Ar$ ages from the samples from the Keis Supergroup of the Kheis Terrane that suggests an Eburnean age (~1.8Ga, Cornell *et al*., 1998 and Moen, 1999) for the origin of the Kheis Terrane. Therefore it could either be argued that the Kheis orogeny never took place at ~1.8Ga or that the thermal event represented by the ~1104Ma to 1113Ma $^{40}Ar/^{39}Ar$ ages (Figure 4.4), obtained from metamorphic muscovite from the Goedehoop Formation and the Kheis Terrane, was of such a big scale that any evidence for the occurrence of the Kheis orogeny at that time was obliterated. Other techniques and evidence should therefore be utilised to further investigate the existence or timing of the Kheis orogeny.

4.5 CONCLUSIONS

The collision of the Kakamas Terrane with the western margin of the Kaapvaal-Zimbabwe craton only took place after deposition of the Puntsit- and Goedehoop Formations at around

1113Ma ago as indicated by the age of syntectonic muscovite in both the Kakamas and Kheis Terranes. Furthermore, $^{40}Ar/^{39}Ar$ dating did not provide any evidence for the formation of the Kheis Terrane at ~1.8Ga ago.

4.6 REFERENCES

Cornell, D.H., Armstrong, R.A. and Walrafen, F., (1998): Geochronology of the Proterozoic Hartley Basalt Formation, South Africa: constraints on the Kheis tectonogenesis and the Kaapvaal Craton's earliest Wilson Cycle. *Jour. Afr. Earth Sci*., **26(1)**, 5-27

Dalziel, I.W.D., Mosher, S. and Gahagan, L.M., (2000): Laurentia-Kalahari collision and the assembly of Rodinia. *J. Geol*., **108**, 499-513

Jacobs, J., Ahrendt, H., Kreutzer, H. and Weber, K., (1995): K-Ar, $^{40}Ar/^{39}Ar$ and apatite fission-track evidence for Neoproterozoic and Mesozoic basement rejuvenation events in the Heimefrontfjella and Mannefallknausane (East Antarctica). *Precambrian. Res*., **75**, 251-262

Jacobs, J., Falter, M., Thomas, R.J., Kunz, J. and Jeßberger, E.K., (1997): $^{40}Ar/^{39}Ar$ Thermochronological constraints on the structural evolution of the Mesoproterozoic Natal Metamorphic Province, SE Africa. *Precambrian. Res*., **86**, 71-92

Jacobs, J. and Thomas R.J., (1996): Pan-African rejuvenation of the ~1.1Ga Natal Metamorphic Province: K/Ar muscovite and titanite fission-track evidence. *J. Geol. Soc. Lond.*, **153**, 971-978

Moen, H.F.G., (1999): The Kheis Tectonic Subprovince, southern Africa: A lithostratigraphic perspective. *S. Afr. J. Geol*., **102(1)**, 27-42

Moores, E.M., (1991): Southwest U.S.-East Antarctic (SWEAT) connection: a hypothesis. *Geology*, **19**, 425-428

Steiger, R.H. and Jäger, E., (1978): Subcommission on Geochronology; convention on the use of decay constants in geochronology and cosmochronology. In: *Contributions to the geologic time scale* G.V. Cohee, M.F Glaessner, and H.D Hedberg, eds), Studies in Geology , Tulsa, **6**, 67-71

Thomas, R.J., Cornell, D.H., Moore, J.M. and Jacobs, J., (1994): Crustal evolution of the Namaqua-Natal Metamorphic province, southern Africa. *S. Afr. J. Geol*., **97(1)**, 8-14

Vasconselos, P. M., Onoe, A.T., Kawashita, K., Soares, A. J. and Teixeira, W., (2002): $^{40}Ar/^{39}Ar$ geochronology at the Instituto de Geociências, USP: instrumentation, analytical procedures, and calibration. *Ann. Brazilian Academy of Sciences,* **74(2)**, 297-342

Zheng, Y.F, Zhao, Z.F., Li, S.G. and Gong, B. (2003): Oxygen isotope equilibrium between ultrahigh-pressure metamorphic minerals and its constraints on Sm-Nd and Rb-Sr chronometers. *In*: Vance D., Muller, W. and Villa, I.M.. (Eds.), *Geochronology: Linking the Isotopic record with petrology and textures*. Spec. Publ., Geol. Soc.., **220**, 93-118